Title

Molecular Programming of Tumor-Infiltrating CD8+ T Cells and IL15 Resistance

Journal

Cancer Immunology Research, 4(9)

ISSN

2326-6066

Authors

Doedens, Andrew L
Rubinstein, Mark P
Gross, Emilie T
et al.

Publication Date

2016-09-02

DOI

10.1158/2326-6066.cir-15-0178

Peer reviewed

HHS Public Access

Author manuscript

Cancer Immunol Res. Author manuscript; available in PMC 2017 September 02.

Published in final edited form as:

Cancer Immunol Res. 2016 September 2; 4(9): 799–811. doi:10.1158/2326-6066.CIR-15-0178.

Molecular programming of tumor-infiltrating CD8+ T cells and IL15 resistance

Andrew L. Doedens[1], **Mark P. Rubinstein**[1,2], **Emilie T. Gross**[3], **J. Adam Best**[1], **David H. Craig**[2], **Megan K. Baker**[2], **David J. Cole**[2], **Jack D. Bui**[3], and **Ananda W. Goldrath**[1]

[1]Division of Biological Sciences, University of California, San Diego, CA USA

[2]Department of Surgery, Medical University of South Carolina, Charleston, SC USA

[3]Department of Pathology, University of California, San Diego, CA USA

Abstract

Despite clinical potential and recent advances, durable immunotherapeutic ablation of solid tumors is not routinely achieved. IL15 expands NK, NKT, and $CD8^+$ T-cell numbers and engages the cytotoxic program, and thus is under evaluation for potentiation of cancer immunotherapy. We found that short-term therapy with IL15 bound to soluble IL15 receptor α–Fc (IL15cx; a form of IL15 with increased half-life and activity) was ineffective in the treatment of autochthonous PyMT murine mammary tumors, despite abundant $CD8^+$ T-cell infiltration. Probing of this poor responsiveness revealed that IL15cx only weakly activated intratumoral $CD8^+$ T cells, even though cells in the lung and spleen were activated and dramatically expanded. Tumor-infiltrating $CD8^+$ T cells exhibited cell-extrinsic and cell-intrinsic resistance to IL15. Our data showed that in the case of persistent viral or tumor antigen, single-agent systemic IL15cx treatment primarily expanded antigen-irrelevant or extratumoral $CD8^+$ T cells. We identified exhaustion, tissue-resident memory, and tumor-specific molecules expressed in tumor-infiltrating $CD8^+$ T cells, which may allow therapeutic targeting or programming of specific subsets to evade loss of function and cytokine resistance, and in turn, increase the efficacy of IL2/15 adjuvant cytokine therapy.

Keywords

animal models of cancer; breast cancer; lymphokines; cytokines; chemokines; growth factors; tumor resistance to immune factors; $CD8^+$ T cells; IL15

Introduction

Antigen-specific immunity to intracellular pathogens requires $CD8^+$ T cells. Inducing $CD8^+$ T cells to mount a response against cancer cells with the same specificity and efficacy as they do against pathogen-infected cells is a long-sought goal of immunotherapy. One method to increase immune responses to cancer is to administer T cell–trophic/activating cytokines, such as IL2 (1). IL15 is closely related to IL2, and expands/activates $CD8^+$ T cells, NK and NKT cells (2,3). Relative to IL2, IL15 results in less expansion of regulatory

agoldrath@ucsd.edu, Address: 9500 Gilman Drive, La Jolla CA 92037.

T cells, as it signals independent of IL2Rα, and IL15 has been identified as a strong candidate for clinical translation (4,5). IL15 half-life/activity is greatly enhanced when complexed with a soluble IL15 receptor α chain coupled to an Fc fragment (IL15cx) (6,7). IL15cx has shown promise in some cancer models (6-10) and is in clinical trials for treatment of melanoma and multiple myeloma.

Upon exposure to persistent viral antigen, $CD8^+$ T cells become 'exhausted', undergoing a progressive and hierarchical loss of function, and up-regulate numerous receptors that inhibit T-cell activation, including PD-1; a process which may serve to limit immunopathology (11,12). Exhaustion plays a role in the molecular programming of tumor-specific $CD8^+$ T cells (13-15), and PD-1 blockade increases $CD8^+$ T-cell responses to chronic viral or tumor antigen (16,17). In addition to TCR-mediated signals, T-cell activation by common γ-chain cytokines (such as IL2 and IL15) also induces proliferation and activation of the cytotoxic program (2). If exhaustion evolved as a mechanism of peripheral tolerance to limit host immunopathology, it may do so at multiple levels, including TCR- and cytokine-mediated activation. From this perspective, inhibitory receptors like PD-1 may dampen TCR-mediated cytotoxicity, whereas a parallel program of exhaustion-induced cytokine resistance may limit the abundance of antigen-specific T cells and their acquisition of cytotoxic phenotypes via TCR-independent cytokine signaling. The mechanisms underlying exhaustion-induced cytokine resistance are poorly understood.

Despite screening and current treatments, mammary cancer results in ~40,000 deaths annually in the US. The transgenic, autochthonous PyMT model of mammary carcinogenesis reproduces important aspects of human breast cancer, including stage-wise histological progression (18). Upon observing marked $CD8^+$ T-cell infiltration of tumors in the PyMT model, we hypothesized that activation and expansion of the abundant $CD8^+$ infiltrate with IL15cx would promote regression of PyMT tumors. We found, however, that PyMT mammary tumor growth was not affected in the short-term by daily treatment with IL15cx, due to tumor-mediated extrinsic and T cell-intrinsic resistance to IL15, even when combined with PD-L1 blockade. We use the PyMT model and integration of multiple datasets to determine the molecular programming of IL15-resistant, tumor-infiltrating $CD8^+$ T cells.

Materials and Methods

PyMT model and LCMV infections

Mice were bred/housed in specific pathogen-free conditions in accordance with the Institutional Animal Care and Use Committee guidelines of UCSD. Female C57BL/6J, or MMTV-$PyMT^{+/-}$ mice (18,19) backcrossed to C57BL/6J (hereafter referred to as "PyMT") (20), were used for all studies. After tumors were measurable on PyMT mice at ~16-24 weeks of age, mice were randomly assigned to control or experimental groups. Tumor volumes were similar between groups before treatment. Volumes of measurable tumors (between 10 and 1000 mm^3) were calculated with the formula V=1/2(A*A*B), where A is larger of two 90-degree caliper measurements. For PyMT MEC studies, 10^5 cells of a PyMT mammary epithelial cell line (Py230, provided by Dr. Lesley Ellies, UCSD) mixed 1:1 with Matrigel (BD Biosciences) were injected into the #4 mammary gland, and allowed to

establish in female mice for 4-8 weeks. Py230 were pathogen-negative by Impact III PCR (Idexx Bioresearch), were obtained in 2014, and demonstrated uniform 'cobblestone' epithelial cell morphology (observed by A.L.D.). Acute and persistent LCMV infections performed as in refs. (16,21). Tumor single-cell suspensions were generated by chopping, 0.05% collagenase D (Roche Diagnostics) incubation, and 20 μm straining, as in ref.(22). Spleens were disrupted with frosted glass slides and then treated identically as tumor samples.

Cell culture and cytokines

Cells were cultured in RPMI 1640, 10% FBS, 10 U/mL penicillin/streptomycin, 40mM HEPES and 55 μM β-mercaptoethanol (Life Technologies), with hIL2 or hIL15 where indicated (NCI Preclinical Repository). Anti-CD3/anti-CD28 activation was performed as in (21). One dose of IL15cx was generated by incubating 0.5 μg hIL15 with 2.3μg sIL15Rα-Fc (R&D systems) in PBS at 37°C for 15m, and injected *ip* in 200 μl PBS.

Cell sorting, microarray and microscopy

For microarray, single-cell suspensions were double-sorted (FACS Aria, BD Biosciences), biological triplicates of $CD8^+CD44^{high}$ cells from the spleen and tumor, excluding MHC II, CD4, B220 or propidium iodide positive cells. RNA/microarray processing can be found at www.immgen.org. Microarray/GSEA/Multiplot analyses was performed at www.genepattern.org; gene expression calculated by RMA. DAVID (23) and Metascape (24) were used to identify targets rather than as a stringent enrichment test. CD8 (53-6.7; eBioscience) was detected with alkaline phosphatase on 10 μm frozen sections counterstained with nuclear fast red (Vector Labs). For Fig. 5B-C, fold change was calculated as follows: $CD103^+$ T_{RM}: $CD103^+$ brain vs. $CD103^-$ spleen (OT-I / VSV-OVA day 20, GSE39152). $CD103^-$ T_{RM}: $CD103^+$ brain vs. $CD103^-$ brain (OT-I / VSV-OVA day 20, GSE39152). T_{REG}: $FOXP3^+$ vs. $FOXP3^-$ splenic $CD4^+$ T cells (GSE15907); $KLRG1^{high}$: $KLRG1^{high}$ vs. $KLRG1^{low}$ P14 cells (LCMV-Arm day 8, GSE46025); PD-1^{high}: $TCR\beta^+CD8^+NK1.1^{neg}PD1^{high}$ vs. $TCR\beta^+CD8^+NK1.1^{neg}PD1^{low}$, and $TCR\beta^+NK1.1^+$: $TCR\beta^+CD8^+NK1.1^{pos}PD1^{low}$ vs. $TCR\beta^+CD8^+NK1.1^{neg}PD1^{low}$ (PyMT tumor populations, GSE76362, count data processed with DEseq2 (25)).

Flow cytometry

Immunostaining was performed with antibodies against CD8α (53-6.7), CD25 (PC61.5), CD43 (eBioR2/60), CD44 (IM7), CD69 (H1.2F3), CD71 (R17217), CD122 (TM-B1), CD127 (A7R34), CD103 (2E7), CD200R (OX110), CD244 (244F4), CXCR3 (CXCR3-173), GITR (DTA-1), EOMES (Dan11mag), KLRG1 (2F1), LAG-3 (C9B7W), Ly6C (HK1.4), IKZF2/HELIOS (22F6), PD-1 (J43), PD-L1 (MIH5), TBET (4B10), TOX (TXRX10), all from eBioscience; GZMB (MHGB05) from Life Technologies, and TCF1 (C63D9) from Cell Signaling Technologies. LCMV-gp33-41 virus-specific $CD8^+$ T cells were identified with MHC I tetramers (Beckman Coulter).

Results

Short-term IL15cx treatment fails to affect tumor volume

All ten mammary glands in female PyMT mice develop tumors of mixed size and histological progression by 3-4 months of age on the C57BL/6J background (18). Immunohistochemistry and flow cytometry of single-cell suspensions of the tumors revealed a high CD8:CD4 ratio, $CD8^+CD44^{high}$ T-cell infiltrate (Fig. 1A,B). PyMT mice were randomly assigned to two groups and administered vehicle or IL15cx for five days (Fig. 1C). We observed activated $CD8^+$ T cells and upregulated expression of cytotoxic molecules in the spleens of the PyMT mice (Supplementary Fig. S1A and B), yet we detected no increased tumor regression or halting of tumor growth due to IL15cx treatment over the five-day experiment (Fig. 1D). Extending treatment over two weeks did not significantly change tumor volumes (data not shown). Intrigued by the extensive infiltration of PyMT tumors with $CD8^+$ T cells with no objective IL15-induced effect on tumor volume, we further investigated tumor-infiltrating $CD8^+$ T cell responsiveness to IL15.

Tumor-infiltrating $CD8^+$ T-cell IL15cx resistance

We first determined whether PyMT mice had systemic, global suppression of T-cell responsiveness to IL15cx, or a local, tumor-specific resistance. We analyzed $CD8^+$ T cells from spleen, lung, and tumors of PyMT mice (vehicle and IL15-treated, as in Fig. 1C). The treatment regimen expanded $CD8^+$ T-cell absolute numbers in the spleen (Fig. 1E), but not in tumors (Fig. 1F; $P = 0.64$ by Student's unpaired t test); $CD8^+$ T cell relative abundance (%) increased 4.5-fold in the spleen and 7-fold in the lung, whereas tumors failed to show an increase (Fig. 1G). The experiments in Fig. 1E-G and Supplementary Fig. S1A and B were all performed in PyMT mice, precluding global suppression of IL15cx signaling in tumor-bearing mice as a mechanism for poor intratumoral IL15cx activity.

We measured expression of GZMB in the tumor and a non-lymphoid tissue, to determine if IL15cx was driving acquisition of a cytotoxic profile in the periphery (Fig. 2A). $CD8^+$ T cells from the lungs of vehicle-treated animals were largely negative for GZMB, consistent with a resting/non-effector phenotype. In the IL15cx treatment group, nearly all lung $CD8^+$ T cells had up-regulated GZMB (Fig. 2A). However, only half of $CD8^+$ T cells isolated from PyMT tumors up-regulated GZMB after IL15cx treatment (Fig. 2A). Thus, resistance to IL15cx is tumor-specific, and blocked increases in $CD8^+$ T cell number, percentage, and cytotoxic phenotype. .

Extrinsic and intrinsic resistance to IL15 by tumor $CD8^+$ T cells

T cells can be suppressed by tumors via multiple mechanisms (for example, refs.(22,26)); we tested whether IL15 resistance was dependent on the tumor environment, and thus cell-extrinsic, or if the resistance was a property of the T cells, and thus cell-intrinsic. Tumor single-cell suspensions were cultured *in vitro* for three days with or without IL15. The transferrin receptor (CD71) is an established lymphocyte activation marker (27) that correlates with GZMB protein up-regulation after IL15 treatment (data not shown). High concentrations of IL15 (1 μg/mL) for three days did not activate the $CD8^+$ T cells within the PyMT tumor single-cell suspension, whereas separately cultured splenic $CD8^+$ T cells

uniformly up-regulated CD71 in response to IL15 (Supplementary Fig. S2A). Furthermore, PyMT single-cell suspensions suppressed the cytokine responsiveness of WT splenocytes in a dose-dependent fashion (Supplementary Fig. S2B and C).Thus, T cell-extrinsic, tumor-mediated mechanisms of suppression were in part limiting T-cell activation.

To determine if intratumoral $CD8^+$ T cells also exhibited cell-intrinsic resistance to IL15, we sort-purified $CD8^+$ T cells from tumor suspensions, as well as splenic $CD8^+$ T cells as a positive control, and tested their responsiveness to IL15 *in vitro*. Only ~50% of the tumor-derived, sort-purified $CD8^+$ T cells responded to IL15, even after incubation in tumor cell-free media for three days with an excess of IL15 (1 μg/mL; Fig. 2B,C). We also observed a defect in accumulation after anti-CD3/anti-CD28 stimulation, further indicating hypo-responsiveness of PyMT tumor-infiltrating $CD8^+$ T cells (Fig. 2C). We then focused on what molecular programs underlie the cell-intrinsic component of $CD8^+$ T-cell resistance to IL15.

Exhausted tumor $CD8^+$ T cell signature despite ample effector transcripts

We isolated PyMT tumor $CD8^+$ cells and control splenic $CD8^+$ T cells, and performed microarray analysis alongside samples of the Immunological Genome Project, Immgen (28). First, we tested the hypothesis that poor $CD8^+$ T-cell antitumor activity in the PyMT model is a result of failure to initiate or sustain the cytotoxic effector program. Contrary to our hypothesis, we found abundant transcripts associated with CTL effector differentiation and function in PyMT tumor T cells, including granzyme family members differentiation factors essential for effector differentiation including *Tbx21*(TBET), *Id2* and *Prdm1* (BLIMP1). The relative expression of GZMB mRNA in PyMT tumor $CD8^+$ T cells was nearly as high as that expressed in $CD8^+$ effector T cells near the peak of the cellular response to *Listeria monocytogenes*-OVA infection (Fig. 3B) (29). Thus, the lack of $CD8^+$ T-cell antitumor activity is not explained by a lack of transcripts coding for effector programming or cytotoxic mediators. The abundant GZMB mRNA (Fig. 3A and B) was not reflected in protein expression in PyMT tumor $CD8^+$ T cells (Fig. 2A).

To exclude that the absence of cytokine receptors caused the poor PyMT $CD8^+$ T-cell response to IL15cx, we characterized gene expression and protein abundance of IL2 and IL15 receptors on PyMT tumor $CD8^+$ T cells: we find PyMT tumor $CD8^+$ T cells expressed abundant receptor molecules for IL15cx (Supplementary Fig. S3A-C; further characterization in Supplementary Fig. S3D and E).

We then tested PyMT tumor $CD8^+$ T cells vs. those responding to acute infection with vesicular stomatitis virus-OVA (VSV-OVA, day 8) for gene-set enrichment using GSEA (30). The top gene set (S) returned was persistent versus acute infection (GSE30962), with a normalized enrichment score of 3.25 (Fig.3C, Supplementary Fig. S4). This result links the PyMT tumor $CD8^+$ T-cell gene signature with that of chronic vs acute viral infection. As a resource, we present PyMT tumor $CD8^+$ T-cell gene expression relative to Immgen datasets for $CD8^+$ T cells from naïve and post-infection populations (Supplementary Fig. S5 and Supplementary Tab. S1-4).

To further explore the contribution of T-cell exhaustion to tumor T-cell programming, we plotted fold change versus *P*-value of the gene-expression data from PyMT tumor versus

splenic $CD8^+CD44^{high}$ T cells, and highlighted genes differentially expressed in persistent versus acute LCMV infection (GSE41870 and ref. (31)). The transcripts differentially regulated by PyMT tumor compared to splenic $CD8^+$ T cells shared ~80% identity with genes up or down in persistent versus acute infection (Fig. 3D). Exhaustion-associated cell-surface markers (32) were also highly expressed (Fig. 3E).

To validate the gene-expression data linking exhaustion to the PyMT tumor $CD8^+$ T-cell phenotype, and further characterize their activation state, we directly compared the cell-surface protein abundance of exhaustion-associated markers on PyMT tumor $CD8^+$ T cells with virus-specific $CD8^+$ T cells in acute or persistent infection. We found marked up-regulation of PD-1, PD-L1, LAG3, CD244, CD69, and CD43 expression on both tumor-infiltrating $CD8^+$ T cells and those from chronic viral infection, but not on those from acute viral infection or uninfected mice (Fig. 3F). In many cases these markers were more abundant on the PyMT tumor $CD8^+$ T cells than those from persistent viral infection. To test how results in the PyMT murine model of breast cancer compared to human disease, we performed flow cytometry on $CD8^+$ T cells infiltrating human breast cancers versus control peripheral samples (Supplementary Fig. S6). We found human breast cancer-associated $CD8^+$ T cells to highly express CD69, PD-1, and CD244.

To identify how $CD8^+$ T cell transcription varied from competent $CD8^+$ T cells versus those in PyMT tumors, we plotted gene expression in $CD8^+$ T cells in response to VSV-OVA infection and PyMT tumor (Fig. 3G; tabular data in Supplementary Tab. S5). We then highlighted genes regulated ≥2-fold in persistent infection (GSE41870) and in $CD8^+$ T cells infiltrating B16 melanomas (GSE15907). This plot demonstrates T-cell activation in tumors or during infection similarly regulates many genes, which appear along the 45-degree axis line. In addition, the highlighting illustrates multiple transcripts regulated in PyMT tumor $CD8^+$ T cells are similarly regulated in B16 melanoma tumor $CD8^+$ T cells, and to a lesser degree, in response to infection. These include up-regulation of effector molecule *Gzmb* and the phosphatase *PtPrj*, and the down-regulation of transcription factor *Myb*. Despite similarities, tumors and acute infection up- and down-regulate specific subsets of genes, such as the tumor- and persistent virus-specific up-regulation of *Cd200r1*, or the acute and persistent infection-specific up-regulation of *Itgam* (Fig.3G). Therefore, although the T-cell exhaustion program is a major contributor to tumor $CD8^+$ T-cell gene expression, there remain a small number of tumor- and virus-specific genes. We wondered what factors or differentiation pathways might be responsible for genes regulated in tumor, but not in the acute or persistent infection datasets.

A subset of tumor $CD8^+$ T cells up-regulate a resident memory T-cell gene-expression signature

A $CD8^+$ T-cell memory subset residing in tissues (33), called tissue-resident memory T cells (T_{RM}), typically expresses *Itgae* (CD103) and *Cd69*, along with a set of other transcripts including *Cdh1* (E-cadherin) (34). PyMT tumor $CD8^+$ T cells expressed multiple transcripts associated with T_{RM} cells, including CD103. Using the "core" T_{RM} signature (34), PyMT tumor $CD8^+$ T cells similarly up- or down-regulate ~80 percent of the transcripts versus splenic controls (Fig. 4A). We further compared our PyMT tumor $CD8^+$ T-cell data with

gene-expression data of brain CD103$^+$ T_{RM} versus conventional splenic memory T cells (35) and persistent versus acute viral infection (31) (Supplementary Fig. S7A). Again, PyMT tumor CD8$^+$ T cells express many T_{RM} transcripts, with few shared with exhausted cells, such as *Chn2* and *Cd244* (Supplementary Fig. S7A). Thus, both an exhausted and T_{RM} gene-expression signature are present in the PyMT tumor CD8$^+$ T-cell population. We then plotted the transcription factors/regulators differentially expressed ≥2-fold between PyMT tumor versus spleen CD8$^+$ T cells, where exhaustion and T_{RM} programming appear to explain much of the gene expression in PyMT tumor CD8$^+$ T cells (Fig. 4B).

To distinguish whether PyMT tumor CD8$^+$ T cells have a mixed differentiation comprising exhausted and T_{RM}-like cells, all within a uniform population, or whether PyMT tumor CD8$^+$ T cells consist of a mixture of distinct exhausted and T_{RM}-like cells, we immunostained CD103, CD69, and PD-1 on PyMT tumor CD8$^+$ T cells (Fig. 4C), using a slow-growing PyMT mammary epithelial cancer cell line (PyMT MEC) injected into mammary glands of female mice. We found that CD103 and PD-1 were largely mutually exclusive, while CD69 was expressed at a moderate level on PD-1^{high} cells. This result suggests that T_{RM}-like and exhausted cells were two different tumor-infiltrating subsets in PyMT MEC tumors, which can be distinguished with CD103 and PD-1.

Molecular Characterization of IL15-Resistant Population

Transcription factors/regulators play central roles in lymphocyte programming (36). T-box transcription factors TBET and EOMES play non-redundant, essential roles in CD8$^+$ effector T-cell differentiation, whereas TCF1 is required for normal thymic T-cell development and memory cells, but is markedly down-regulated in effector CD8$^+$ T cells (29,36). Many T_{REG} highly express IKZF2/HELIOS, which is essential for full suppressive function (37); this factor is absent from splenic CD8$^+$ T cells (29). TOX is an HMG-box factor essential for T-cell development (38) with an unknown role in peripheral T cells. To further characterize the exhausted and T_{RM}-like infiltrate, we assessed protein levels of transcription factors/regulators found to be regulated in the PyMT transcript-expression data: *Tox* was one of the most differentially regulated, and was associated with exhausted, but not T_{RM}-like, cells (Fig. 4B). We distinguished the T_{RM}-like and exhausted subsets with PD-1 and CD103, and immunostained for transcription factors/regulators TBET, TCF1 (product of *Tcf7*), IKZF2/HELIOS, TOX and EOMES (Fig. 4D). The exhausted subset, using PD-1 as a marker, was always TOX^{high}, TCF1^{low}, EOMES^{low}, and intermediate for IKZF2 (Fig. 4D*)*. We found that CD103$^+$ cells, correlated with the T_{RM}-like subset, were TOX negative, and had mixed IKZF2 expression and intermediate-high TBET (Fig. 4D). As in Fig.4C, these data further suggest there is a distinct CD103$^+$ T_{RM}-like component of the PyMT MEC tumor CD8$^+$ T-cell population that does not exhibit high PD-1 or TOX.

We previously observed cell-intrinsic IL15 resistance in a subset of tumor CD8$^+$ T cells (Fig. 2). Having established T_{RM}-like and exhausted subsets in the tumor, we then determined their IL15 responsiveness. First, we determined that IL15 receptors CD122 and CD132 were similarly expressed on PD-1 high and low tumor-infiltrating CD8$^+$ T cells (Supplementary Fig. S3C). We then sorted PyMT MEC tumor T cells based on CD103 expression and splenocytes as a control, and cultured with or without IL15 for 60 hours (Supplementary

Fig. S7B). The splenic CD8$^+$ T cells responded to IL15 culture with near uniform up-regulation of CD71 and were >97% negative for IKZF2, TOX and PD-1 (Supplementary Fig. S7B). In contrast, a subset of sorted tumor CD8$^+$ T cells did not up-regulate CD71, as was previously observed in Fig. 2B. We found that the CD71^{low} cells were almost entirely PD-1^{high}TOX^{high}, and exhibited low side scatter, suggesting a failure to proliferate. CD103^{high} cells were less likely to be PD-1^{high} after IL15 treatment (Supplementary Fig. S7B), as was observed previously in untreated PyMT tumor CD8$^+$ T cells (Fig.4C). We found that the CD103^{pos} tumor-infiltrating cells were more likely to appear IKZF2^{pos}CD71^{high} after IL15 culture: 45% of the sorted CD103$^+$ appeared IKZF2^{high}CD71^{high} versus 14% from the sorted CD103^{neg} population. Taken together, these data indicate the PD-1^{high}TOX^{high} tumor-infiltrating population exhibits a failure to induce blastogenesis in response to IL15. IKZF2 was not predictive of cytokine responsiveness, but was enriched in sorted IL15-treated CD103^{pos} T cells from the tumor.

Given that the IL15-resistant tumor CD8$^+$ T-cell population resembled exhausted CTL responding to persistent viral infection, we wondered whether IL15cx would also fail to expand PD-1^{pos} cells in persistent viral infection with LCMV-cl13. Although IL15cx did result in a dramatic expansion of CD8$^+$ T cells, virus-specific cells were vastly under-represented in the expanded population (Supplementary Fig. S8A and B). This result is unlikely to be explained by cytokine receptors, as *IL2rb* (CD122) and *Il2rg* (CD132) are expressed by virus-specific cells in persistent infection (Supplementary Fig. S3D). *In vitro*, only the PD-1^{low} subset from LCMV-cl13-infected mice exhibited hallmarks of activation after IL15 treatment (Supplementary Fig. S8C), similar to that observed in PyMT tumor CD8$^+$ T cells stimulated with IL15 (Supplementary Fig. S7B). Therefore, these results extend those of previous reports (39) and demonstrate virally-exhausted CD8$^+$ T cells are poorly responsive to IL15 *in vitro* and *in vivo*.

Blockade of PD-1 enhances adaptive immune responses to persistent antigen such as cancer and LCMV-cl13 infection (16). However, cytokine resistance may not be directly addressed by PD-1 pathway blockade; indeed, when administered to PyMT mice, systemic *in vivo* anti-PD-L1 increased the % of intratumoral CD8$^+$ T cells producing IFNγ, but did not affect cytokine resistance as gauged GZMB protein expression or tumor volume in our short-term assay (Supplementary Fig. S9A-D). Therefore, overcoming exhaustion-associated, cell-intrinsic cytokine resistance may require therapeutic strategies beyond PD-L1 blockade.

Targeting regulators of tumor CD8$^+$ T-cell responsiveness and function

To identify novel regulators of tumor-infiltrating CD8$^+$ T cells, we returned to the gene-expression data (Fig. 3,4): we found 504 genes with increased and 358 with decreased abundance in PyMT CD8$^+$ T cells versus spleen (Fig. 5A; Supplementary Tab. S6 and 7). We collated results from DAVID (23), which determines enrichment among ontology, localization, and other properties (Table 1). We then incorporated additional datasets profiling exhausted CD8$^+$ T cells exposed to persistent antigen: chronic viral infection (GSE41870) and PD1^{high} tumor-infiltrating T cells (GSE76362). Metascape (24) was then used to perform ontological meta-analysis of all three datasets, and the overlap of genes up-regulated 2-fold was diagrammed in Fig. 5A. We focused on three classes of genes:

transcription factors and regulators which may program the exhausted state, signaling regulators potentially underlying exhaustion-induced trophic cytokine resistance, and accessible cell-surface/membrane proteins to reverse T-cell dysfunction. For the selected candidates, we present gene expression data from multiple datasets of T-cell differentiation (Fig. 5B).

We first focused on cell-surface/membrane-localized and immunoglobulin-like domain-containing transcripts (Table 1): these included known exhaustion-associated negative regulators such as *Pdcd1* (PD-1) and *Tigit* (40), as well as *Cd200r1* and myeloid-associated *Cd80* (Supplementary Fig. S10), and T_{RM}-associated adenosine receptor *Adora3*. Expression data for exemplar transcript *Pdcd1* as well as *Lilrb4* and *CD200r1* are presented in Figure 5B. *Lilrb4* is an ITIM-containing negative regulator of immunity (41), and we verified elevated CD200R on PD-1^{high} PyMT tumor T cells beyond that observed in persistent viral infection (Supplementary Fig. S10). *CD200r1* is induced in both $PD1^{high}$ and $NK1.1^{high}$ PyMT tumor subsets (Fig. 5B); CD200R down-regulates TNF in macrophages (42).

Tumor-infiltrating $CD8^+$ T cells exhibit a unique profile of transcription factors and regulators. We selected six transcription factors/regulators to profile: *Tox, Bhlhe40, Ikzf2, Atxn1, Trps1 and Setbp1* (Fig. 5B). Co-expressed TOX and PD-1 correlated with IL15 cytokine resistance (Fig. 4D, Supplementary Fig. S7B); further, *Tox* mirrors *Pdcd1* expression in persistent infection (Fig. 5B and ref.(31)), appearing to mark exhausted $CD8^+$ T cells in tumor and viral contexts. *Bhlhe40* is up-regulated in multiple post-activation T-cell subsets (Fig. 5B), and regulates cytokine production (43). *Ikzf2* expression is abundant in exhausted, T_{REG}, and $CD8\alpha^+NK1.1^+$ tumor-infiltrating cells (Fig.5B and ref.(31)), however it poorly correlated with cytokine resistance (Supplementary Fig. S7B). Lastly, three transcription factors/regulators in exhausted, tumor-infiltrating T cells had unexplored roles in T lymphocytes (Fig.5B): *Trps1* is a transcriptional repressor of GATA-regulated genes, *Setbp1* has a role in myeloid cell malignancies (44), and *Atxn1* is a chromatin-binding protein which can repress Notch signaling (45). In summary, our analysis identifies specific transcription factors/regulators expressed in multiple exhausted and tumor-infiltrating $CD8^+$ T cell populations.

We then profiled several clusters with roles in negative regulation of signal transduction or proliferation (Table 1 and Fig. 5B); one such cluster contained *Cish, Rgs1, Rgs3,* and *Rgs16* (Table 1, Fig. 5B). *Cish* is a SOCS and SH2 domain protein, diminishes JAK/STAT signaling (46), and affects tumor-infiltrating $CD8^+$ TCR responsiveness (47). Regulator of G-protein signaling (RGS) molecules control immune cell migration and activation. *Rgs1* is highly expressed in T_{RM} and regulates trafficking (48). *Rgs16* is induced by cell activation, persistent infection and in T_{RM} cells (Fig. 5B), and inhibits immune cell activation (49). Integrins serve adhesion and cell signaling regulatory roles: *Itgav* (Fig. 5B) binds extracellular matrix proteins, including fibronectin and laminin; integrins have been successfully targeted clinically (50). *Samsn1*/*Hacs1/Sly2* (Fig. 5B) is a SH3-containing, immuno-inhibitory adaptor which can bind ITIM's such as those in *Pdcd1* and *Lilrb4*: ablation of *Samsn1* up-regulates cellular tyrosine phosphorylation, while over-expression impedes B/$CD4^+$ T-cell activation/proliferation (51-53). *Glcci1* (Fig. 5B) is induced by anti-

inflammatory glucocorticoids, and in humans, SNPs in *Glcci1* markedly affect response to glucocorticoid therapy in asthma patients (54). *Prr5l* (Fig. 5B) directly binds to mTORC2, and *Prr5l* degradation by RFFL2 results in mTORC2-dependent protein kinase C activation (55,56). Altogether, we find that specific signaling regulators with potent anti-proliferative and immuno-inhibitory functions are up-regulated in exhausted, tumor-infiltrating $CD8^+$ T cells.

Phosphatases can attenuate TCR and cytokine responsiveness; we found *Dusp* and *Ptpn* family members (Table 1, Supplementary Tab. S8), as well as phosphatase subunit *Ppp2r2c* enriched in PyMT $CD8^+$ T cells. We further profiled *Dusp4, Ptpn13* and *Ppp2r2c*:. we observe marked enrichment of these phosphatases in $PD1^{high}$ tumor-infiltrating cells, while IL15-responsive $CD8\alpha^+NK1.1^+$ cells (57) showed minimal enrichment (magenta and orange bars; Fig. 5B).

To facilitate further identification of cell-surface molecules, we used gene ontology and manual identification to select transcripts coding for cell-surface molecules and ordered them by fold change in PyMT tumor $CD8^+$ T cells versus splenic controls (Fig. 5C). We then calculated fold change for multiple $CD8^+$ T-cell datasets and depicted this via heatmap, allowing visualization of shared or differential relative expression in tumor, acute infection (LCMV-Armstrong), persistent infection (LCMV-clone13), T_{RM}, $PD1^+NK1.1^-$ and $NK1.1^+PD1^-$ PyMT tumor-infiltrating $CD8^+$ T cells.

Our strategy of gene-expression profiling has identified potential regulators of tumor-infiltrating $CD8^+$ T cells that may be pursued in future studies as therapeutic targets.

Model of molecular programming of tumor-infiltrating $CD8^+$ T cells and IL15 resistance

PyMT $CD8^+$ T cells exhibit cell-intrinsic resistance to IL15cx therapy correlated with an exhausted phenotype. These data suggest the predominant effect of systemic IL15cx to either tumor-bearing or persistent virus-infected mice was expansion of irrelevant $CD8^+$ T cells (Fig. 6A; flow cytometry-verified molecules summarized in Fig. 6B). We observed that the adoptive transfer of activated tumor-specific $CD8^+$ T cells resulted in rapid induction of exhaustion markers PD-1 and CD244, suggesting exhaustion-induced cytokine resistance will also apply to adoptively transferred cells (Supplementary Fig. S11). As molecules at the cell surface are readily targeted and thus candidates for clinical translation, we present a Venn diagram of cell-surface molecule relative expression in $CD8^+$ T cells exposed to persistent antigen (Fig. 6C).

Discussion

Common gamma-chain cytokines induce $CD8^+$ T-cell activation, proliferation, and cytotoxic programming (2). IL2 is FDA-approved to treat metastatic melanoma (1) and IL15-based therapies are under intense investigation and clinical development. However, we found the PyMT model of mammary carcinogenesis to be refractory to short-term IL15cx-mediated tumor destruction. Tumor-infiltrating $CD8^+$ T cells exhibited extrinsic and intrinsic resistance to IL15: the majority failed to engage cytotoxic and proliferative programs, despite expression of IL2/15 receptors, purification by cell sorting, and extended IL15

treatment *in vitro*. In humans, adjuvant cytokine therapy must be carefully managed to avoid morbidity and mortality (58). Understanding the mechanisms behind cytokine hypo-responsiveness is important to fully and safely exploit common gamma-chain cytokine therapies.

Cancer and persistent viral infection both exhibit high antigen load and the failure of antigen-specific T cells to eliminate the antigen-bearing cells (13). Our analysis confirmed the exhausted phenotype common to both viral and tumor-mediated exhaustion. Previous studies have shown exhausted $CD8^+$ T cells are resistant to gamma chain cytokines (39), yet have also reported their capacity to lower viral titers and partially overcome T-cell exhaustion (recently, ref. (59)). Exhaustion of virus-specific T cells depends on antigen load, and in some cases long-term gamma-chain cytokine administration may lower viral titer indirectly. We observed poor expansion of virus-specific cells by IL15cx (Supplementary Fig. S8).

PD-1^{high}, exhausted phenotype PyMT $CD8^+$ T cells exhibited a specific transcriptional regulator signature: $TOX^{high}TCF7^{low}IKZF2^{med}TBET^{pos}EOMES^{neg}$. We find T_{RM}-like, $CD103^+$ cells to mark a distinct, non-exhausted phenotype population (Fig. 4C,D). CD69 is often used as a T_{RM} marker, yet splenic exhausted cells express CD69 (Fig. 3F and ref.(60)), and PD-1^{high} PyMT MEC tumor $CD8^+$ T cells expressed intermediate CD69 (Fig. 4C), suggesting CD103 may better differentiate T_{RM}-like and exhausted tumor $CD8^+$ T cells. Dadi et al. report a $CD8^+NK1.1^+PD1^-$ tumor-infiltrating population to be cytokine-responsive and often $CD103^+$, calling them "ILTC1" cells (57). Here, we refer to $CD8^+CD103^+PD1^-$ cells as T_{RM}-like, based on T_{RM}-like signature (Fig. 4) and expression of CD103, while Dadi et al. identify the ILTC1 population based in part on NK signature and expression of NK1.1. Both of our reports have found $CD103^+$ cells more likely to be PD-1 negative and to respond to IL15 (Supplementary Fig. S7B). Dadi et al. also found significant delay, but not elimination, of PyMT tumors with transgenic IL15. While we observed no control of tumor volume with IL15cx in our assay, our protocol administered IL15cx to mice with established tumors. Altogether, given the poor response of PyMT tumors to IL15cx despite the presence of ILTC1/T_{RM}-like cells, we conclude targeting of novel regulators of cytokine responsiveness is essential to maximize IL15 anticancer efficacy.

The presence of $CD103^+$, T_{RM}-like $CD8^+$ T cells in tumors may present unappreciated therapeutic opportunities. In our model, $CD8^+CD103^+$ cells appeared less likely to be PD-1^{high} or to express exhaustion-associated transcription factor TOX (Fig. 4D), were more likely to be IL15-responsive (Supplementary Fig. S7B), and expressed unique activation/inhibitory receptors. Further understanding the cytotoxic capacity/activity of $CD103^+$ T_{RM}-like cells in the tumor will inform whether therapeutic strategies should optimally target the cytokine-resistant exhausted cells, T_{RM}-like cells, or both.

Supplementary Material

Refer to Web version on PubMed Central for supplementary material.

Acknowledgements

We acknowledge Jessica Nguyen, Jamie Knell and Jessica Fujimoto for experimental contributions, and Dr. Lesley Ellies for the Py230 cell line.

Financial Support: A.L. Doedens: NIH F32AI082933 and the UCSD Cancer Biology Fellowship; M.P. Rubinstein: NIH R01CA133503; J.D. Bui: NIH R01CA157885 and the Hartwell Foundation Collaboration Award; A.W. Goldrath: NIH R01AI072117 and the Pew Scholars Program.

References

1. Rosenberg SA. IL-2: the first effective immunotherapy for human cancer. Journal of immunology. 2014; 192(12):5451–8.
2. Liu K, Catalfamo M, Li Y, Henkart PA, Weng NP. IL-15 mimics T cell receptor crosslinking in the induction of cellular proliferation, gene expression, and cytotoxicity in CD8+ memory T cells. Proceedings of the National Academy of Sciences of the United States of America. 2002; 99(9): 6192–7. [PubMed: 11972069]
3. Tamang DL, Redelman D, Alves BN, Vollger L, Bethley C, Hudig D. Induction of granzyme B and T cell cytotoxic capacity by IL-2 or IL-15 without antigens: multiclonal responses that are extremely lytic if triggered and short-lived after cytokine withdrawal. Cytokine. 2006; 36(3-4):148–59. [PubMed: 17188506]
4. Cheever MA. Twelve immunotherapy drugs that could cure cancers. Immunological reviews. 2008; 222:357–68. [PubMed: 18364014]
5. Ahmadzadeh M, Rosenberg SA. IL-2 administration increases CD4+ CD25(hi) Foxp3+ regulatory T cells in cancer patients. Blood. 2006; 107(6):2409–14. [PubMed: 16304057]
6. Rubinstein MP, Kovar M, Purton JF, Cho JH, Boyman O, Surh CD, et al. Converting IL-15 to a superagonist by binding to soluble IL-15R{alpha}. Proceedings of the National Academy of Sciences of the United States of America. 2006; 103(24):9166–71. [PubMed: 16757567]
7. Stoklasek TA, Schluns KS, Lefrancois L. Combined IL-15/IL-15Ralpha immunotherapy maximizes IL-15 activity in vivo. Journal of immunology. 2006; 177(9):6072–80.
8. Epardaud M, Elpek KG, Rubinstein MP, Yonekura AR, Bellemare-Pelletier A, Bronson R, et al. Interleukin-15/interleukin-15R alpha complexes promote destruction of established tumors by reviving tumor-resident CD8+ T cells. Cancer research. 2008; 68(8):2972–83. [PubMed: 18413767]
9. Xu W, Jones M, Liu B, Zhu X, Johnson CB, Edwards AC, et al. Efficacy and mechanism-of-action of a novel superagonist interleukin-15: interleukin-15 receptor alphaSu/Fc fusion complex in syngeneic murine models of multiple myeloma. Cancer research. 2013; 73(10):3075–86. [PubMed: 23644531]
10. Mathios D, Park CK, Marcus WD, Alter S, Rhode PR, Jeng EK, et al. Therapeutic administration of IL-15 superagonist complex ALT-803 leads to long-term survival and durable antitumor immune response in a murine glioblastoma model. International journal of cancer Journal international du cancer. 2015
11. Wherry EJ. T cell exhaustion. Nature immunology. 2011; 12(6):492–9. [PubMed: 21739672]
12. Day CL, Kaufmann DE, Kiepiela P, Brown JA, Moodley ES, Reddy S, et al. PD-1 expression on HIV-specific T cells is associated with T-cell exhaustion and disease progression. Nature. 2006; 443(7109):350–4. [PubMed: 16921384]
13. Kim PS, Ahmed R. Features of responding T cells in cancer and chronic infection. Current opinion in immunology. 2010; 22(2):223–30. [PubMed: 20207527]
14. Schietinger A, Greenberg PD. Tolerance and exhaustion: defining mechanisms of T cell dysfunction. Trends in immunology. 2014; 35(2):51–60. [PubMed: 24210163]
15. Baitsch L, Baumgaertner P, Devevre E, Raghav SK, Legat A, Barba L, et al. Exhaustion of tumor-specific CD8(+) T cells in metastases from melanoma patients. The Journal of clinical investigation. 2011; 121(6):2350–60. [PubMed: 21555851]
16. Barber DL, Wherry EJ, Masopust D, Zhu B, Allison JP, Sharpe AH, et al. Restoring function in exhausted CD8 T cells during chronic viral infection. Nature. 2006; 439(7077):682–7. [PubMed: 16382236]

17. Hirano F, Kaneko K, Tamura H, Dong H, Wang S, Ichikawa M, et al. Blockade of B7-H1 and PD-1 by monoclonal antibodies potentiates cancer therapeutic immunity. Cancer research. 2005; 65(3): 1089–96. [PubMed: 15705911]
18. Lin EY, Jones JG, Li P, Zhu L, Whitney KD, Muller WJ, et al. Progression to malignancy in the polyoma middle T oncoprotein mouse breast cancer model provides a reliable model for human diseases. The American journal of pathology. 2003; 163(5):2113–26. [PubMed: 14578209]
19. Guy CT, Cardiff RD, Muller WJ. Induction of mammary tumors by expression of polyomavirus middle T oncogene: a transgenic mouse model for metastatic disease. Molecular and cellular biology. 1992; 12(3):954–61. [PubMed: 1312220]
20. Davie SA, Maglione JE, Manner CK, Young D, Cardiff RD, MacLeod CL, et al. Effects of FVB/NJ and C57Bl/6J strain backgrounds on mammary tumor phenotype in inducible nitric oxide synthase deficient mice. Transgenic research. 2007; 16(2):193–201. [PubMed: 17206489]
21. Doedens AL, Phan AT, Stradner MH, Fujimoto JK, Nguyen JV, Yang E, et al. Hypoxia-inducible factors enhance the effector responses of CD8(+) T cells to persistent antigen. Nature immunology. 2013; 14(11):1173–82. [PubMed: 24076634]
22. Doedens AL, Stockmann C, Rubinstein MP, Liao D, Zhang N, DeNardo DG, et al. Macrophage expression of hypoxia-inducible factor-1 alpha suppresses T-cell function and promotes tumor progression. Cancer research. 2010; 70(19):7465–75. [PubMed: 20841473]
23. Huang da W, Sherman BT, Lempicki RA. Systematic and integrative analysis of large gene lists using DAVID bioinformatics resources. Nature protocols. 2009; 4(1):44–57. [PubMed: 19131956]
24. Tripathi S, Pohl MO, Zhou Y, Rodriguez-Frandsen A, Wang G, Stein DA, et al. Meta- and Orthogonal Integration of Influenza "OMICs" Data Defines a Role for UBR4 in Virus Budding. Cell host & microbe. 2015; 18(6):723–35. [PubMed: 26651948]
25. Love MI, Huber W, Anders S. Moderated estimation of fold change and dispersion for RNA-seq data with DESeq2. Genome biology. 2014; 15(12):550. [PubMed: 25516281]
26. Motz GT, Coukos G. Deciphering and reversing tumor immune suppression. Immunity. 2013; 39(1):61–73. [PubMed: 23890064]
27. Caruso A, Licenziati S, Corulli M, Canaris AD, De Francesco MA, Fiorentini S, et al. Flow cytometric analysis of activation markers on stimulated T cells and their correlation with cell proliferation. Cytometry. 1997; 27(1):71–6. [PubMed: 9000587]
28. Heng TS, Painter MW, Immunological Genome Project C. The Immunological Genome Project: networks of gene expression in immune cells. Nature immunology. 2008; 9(10):1091–4. [PubMed: 18800157]
29. Best JA, Blair DA, Knell J, Yang E, Mayya V, Doedens A, et al. Transcriptional insights into the CD8(+) T cell response to infection and memory T cell formation. Nature immunology. 2013; 14(4):404–12. [PubMed: 23396170]
30. Subramanian A, Tamayo P, Mootha VK, Mukherjee S, Ebert BL, Gillette MA, et al. Gene set enrichment analysis: a knowledge-based approach for interpreting genome-wide expression profiles. Proceedings of the National Academy of Sciences of the United States of America. 2005; 102(43):15545–50. [PubMed: 16199517]
31. Doering TA, Crawford A, Angelosanto JM, Paley MA, Ziegler CG, Wherry EJ. Network analysis reveals centrally connected genes and pathways involved in CD8+ T cell exhaustion versus memory. Immunity. 2012; 37(6):1130–44. [PubMed: 23159438]
32. Blackburn SD, Shin H, Haining WN, Zou T, Workman CJ, Polley A, et al. Coregulation of CD8+ T cell exhaustion by multiple inhibitory receptors during chronic viral infection. Nature immunology. 2009; 10(1):29–37. [PubMed: 19043418]
33. Schenkel JM, Fraser KA, Beura LK, Pauken KE, Vezys V, Masopust D. T cell memory. Resident memory CD8 T cells trigger protective innate and adaptive immune responses. Science. 2014; 346(6205):98–101. [PubMed: 25170049]
34. Mackay LK, Rahimpour A, Ma JZ, Collins N, Stock AT, Hafon ML, et al. The developmental pathway for CD103(+)CD8+ tissue-resident memory T cells of skin. Nature immunology. 2013; 14(12):1294–301. [PubMed: 24162776]

35. Wakim LM, Woodward-Davis A, Liu R, Hu Y, Villadangos J, Smyth G, et al. The molecular signature of tissue resident memory CD8 T cells isolated from the brain. Journal of immunology. 2012; 189(7):3462–71.
36. Cui W, Kaech SM. Generation of effector CD8+ T cells and their conversion to memory T cells. Immunological reviews. 2010; 236:151–66. [PubMed: 20636815]
37. Sebastian M, Lopez-Ocasio M, Metidji A, Rieder SA, Shevach EM, Thornton AM. Helios Controls a Limited Subset of Regulatory T Cell Functions. Journal of immunology. 2016; 196(1):144–55.
38. Wilkinson B, Chen JY, Han P, Rufner KM, Goularte OD, Kaye J. TOX: an HMG box protein implicated in the regulation of thymocyte selection. Nature immunology. 2002; 3(3):272–80. [PubMed: 11850626]
39. Wherry EJ, Barber DL, Kaech SM, Blattman JN, Ahmed R. Antigen-independent memory CD8 T cells do not develop during chronic viral infection. Proceedings of the National Academy of Sciences of the United States of America. 2004; 101(45):16004–9. [PubMed: 15505208]
40. Johnston RJ, Comps-Agrar L, Hackney J, Yu X, Huseni M, Yang Y, et al. The immunoreceptor TIGIT regulates antitumor and antiviral CD8(+) T cell effector function. Cancer cell. 2014; 26(6): 923–37. [PubMed: 25465800]
41. Lu HK, Rentero C, Raftery MJ, Borges L, Bryant K, Tedla N. Leukocyte Ig-like receptor B4 (LILRB4) is a potent inhibitor of FcgammaRI-mediated monocyte activation via dephosphorylation of multiple kinases. The Journal of biological chemistry. 2009; 284(50):34839–48. [PubMed: 19833736]
42. Rygiel TP, Meyaard L. CD200R signaling in tumor tolerance and inflammation: A tricky balance. Current opinion in immunology. 2012; 24(2):233–8. [PubMed: 22264927]
43. Lin CC, Bradstreet TR, Schwarzkopf EA, Sim J, Carrero JA, Chou C, et al. Bhlhe40 controls cytokine production by T cells and is essential for pathogenicity in autoimmune neuroinflammation. Nature communications. 2014; 5:3551.
44. Makishima H, Yoshida K, Nguyen N, Przychodzen B, Sanada M, Okuno Y, et al. Somatic SETBP1 mutations in myeloid malignancies. Nature genetics. 2013; 45(8):942–6. [PubMed: 23832012]
45. Tong X, Gui H, Jin F, Heck BW, Lin P, Ma J, et al. Ataxin-1 and Brother of ataxin-1 are components of the Notch signalling pathway. EMBO reports. 2011; 12(5):428–35. [PubMed: 21475249]
46. Miah MA, Bae YS. Regulation of DC development and DC-mediated T-cell immunity via CISH. Oncoimmunology. 2013; 2(3):e23404. [PubMed: 23802082]
47. Palmer DC, Guittard GC, Franco Z, Crompton JG, Eil RL, Patel SJ, et al. Cish actively silences TCR signaling in CD8+ T cells to maintain tumor tolerance. The Journal of experimental medicine. 2015; 212(12):2095–113. [PubMed: 26527801]
48. Han SB, Moratz C, Huang NN, Kelsall B, Cho H, Shi CS, et al. Rgs1 and Gnai2 regulate the entrance of B lymphocytes into lymph nodes and B cell motility within lymph node follicles. Immunity. 2005; 22(3):343–54. [PubMed: 15780991]
49. Shankar SP, Wilson MS, DiVietro JA, Mentink-Kane MM, Xie Z, Wynn TA, et al. RGS16 attenuates pulmonary Th2/Th17 inflammatory responses. Journal of immunology. 2012; 188(12): 6347–56.
50. Ley K, Rivera-Nieves J, Sandborn WJ, Shattil S. Integrin-based therapeutics: biological basis, clinical use and new drugs. Nature reviews Drug discovery. 2016; 15(3):173–83. [PubMed: 26822833]
51. Wang D, Stewart AK, Zhuang L, Zhu Y, Wang Y, Shi C, et al. Enhanced adaptive immunity in mice lacking the immunoinhibitory adaptor Hacs1. FASEB journal : official publication of the Federation of American Societies for Experimental Biology. 2010; 24(3):947–56. [PubMed: 19923443]
52. Claudio JO, Zhu YX, Benn SJ, Shukla AH, McGlade CJ, Falcioni N, et al. HACS1 encodes a novel SH3-SAM adaptor protein differentially expressed in normal and malignant hematopoietic cells. Oncogene. 2001; 20(38):5373–7. [PubMed: 11536050]
53. von Holleben M, Gohla A, Janssen KP, Iritani BM, Beer-Hammer S. Immunoinhibitory adapter protein Src homology domain 3 lymphocyte protein 2 (SLy2) regulates actin dynamics and B cell spreading. The Journal of biological chemistry. 2011; 286(15):13489–501. [PubMed: 21296879]

54. Tantisira KG, Lasky-Su J, Harada M, Murphy A, Litonjua AA, Himes BE, et al. Genomewide association between GLCCI1 and response to glucocorticoid therapy in asthma. The New England journal of medicine. 2011; 365(13):1173–83. [PubMed: 21991891]

55. Thedieck K, Polak P, Kim ML, Molle KD, Cohen A, Jeno P, et al. PRAS40 and PRR5-like protein are new mTOR interactors that regulate apoptosis. PloS one. 2007; 2(11):e1217. [PubMed: 18030348]

56. Gan X, Wang J, Wang C, Sommer E, Kozasa T, Srinivasula S, et al. PRR5L degradation promotes mTORC2-mediated PKC-delta phosphorylation and cell migration downstream of Galpha12. Nature cell biology. 2012; 14(7):686–96. [PubMed: 22609986]

57. Dadi S, Chhangawala S, Whitlock BM, Franklin RA, Luo CT, Oh SA, et al. Cancer Immunosurveillance by Tissue-Resident Innate Lymphoid Cells and Innate-like T Cells. Cell. 2016; 164(3):365–77. [PubMed: 26806130]

58. Alwan LM, Grossmann K, Sageser D, Van Atta J, Agarwal N, Gilreath JA. Comparison of acute toxicity and mortality after two different dosing regimens of high-dose interleukin-2 for patients with metastatic melanoma. Targeted oncology. 2014; 9(1):63–71. [PubMed: 23609056]

59. West EE, Jin HT, Rasheed AU, Penaloza-Macmaster P, Ha SJ, Tan WG, et al. PD-L1 blockade synergizes with IL-2 therapy in reinvigorating exhausted T cells. The Journal of clinical investigation. 2013; 123(6):2604–15. [PubMed: 23676462]

60. Wherry EJ, Ha SJ, Kaech SM, Haining WN, Sarkar S, Kalia V, et al. Molecular signature of CD8+ T cell exhaustion during chronic viral infection. Immunity. 2007; 27(4):670–84. [PubMed: 17950003]

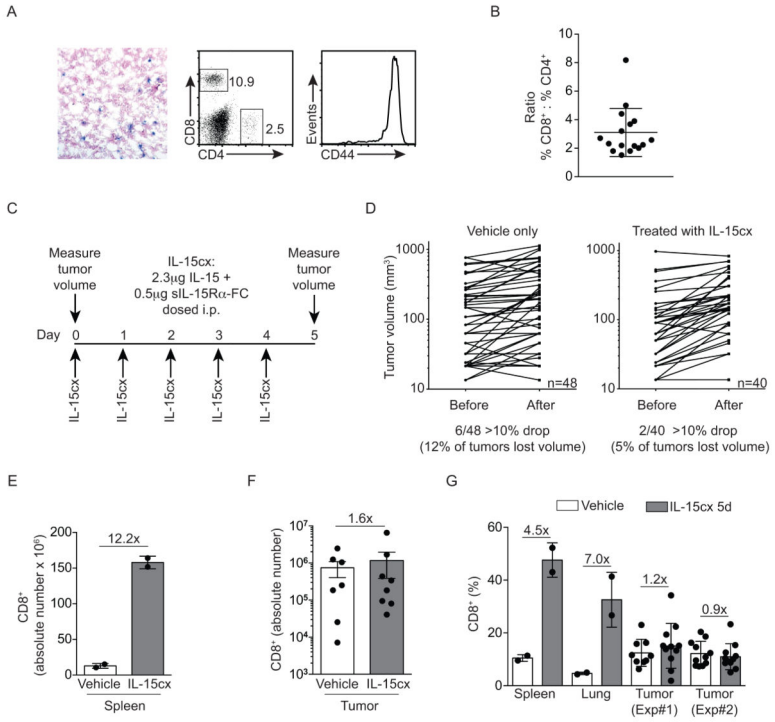

Figure 1. Despite CD8$^+$ T-cell infiltration, PyMT mammary tumors are refractory to immunotherapy with IL15/sIL15Rα cytokine complexes

(A) Left, CD8 immunohistochemistry (blue) from untreated, representative PyMT tumor (nuclei red); middle, flow cytometry of CD4, CD8; and right, CD44 abundance on CD8$^+$ cells from a typical PyMT tumor single-cell suspension. (B) CD8$^+$:CD4$^+$ ratio in single-cell suspensions of untreated PyMT tumors, n=15, error bar S.D. (C) IL15/sIL15Rα cytokine complexes (IL15cx) dosing and tumor measurement schedule. (D). Tumor measurements before and after treatment in C. Each line represents an individual tumor; >10% decrease in volume tallied below (E) Absolute number of CD8$^+$ splenocytes with treatment as in *C*; vehicle and IL15cx treatments are in PyMT mice. Fold expansion indicated above graph; error bars S.D. (F) As in *E*, but measured in single-cell suspensions of PyMT tumors. Error bars S.E.M. (G) Relative abundance (% of live gate) of CD8$^+$ T cells in mice treated as in C. For tumors, results are from two experiments. Fold increase is shown above. Error bars S.D.

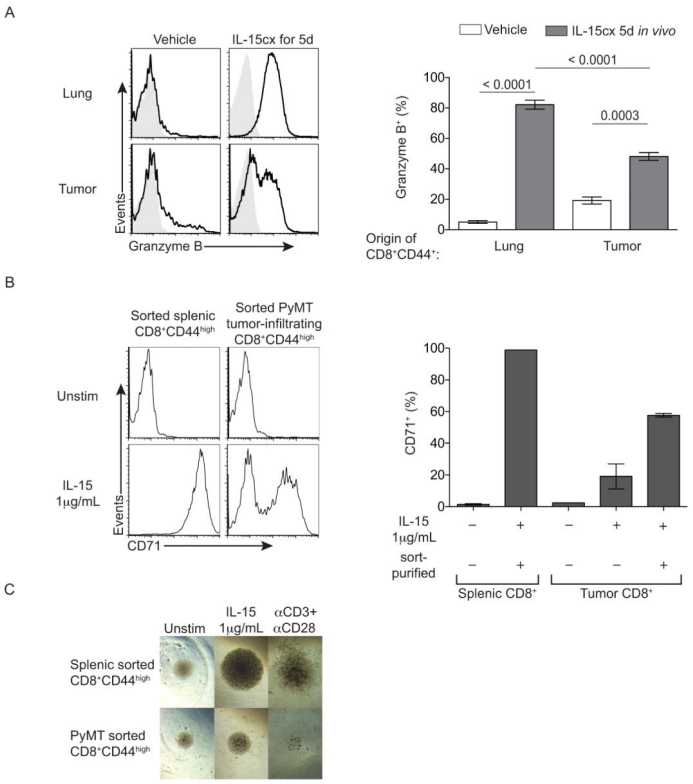

Figure 2. Tumor-infiltrating CD8$^+$ T cells are resistant to IL15-mediated induction of cytotoxic/ proliferation programs *in vivo* and *in vitro*

PyMT tumor-bearing mice dosed as in Fig. 1C. (A) Left, representative lung and tumor CD8$^+$CD44^{high} T-cell GZMB immunostaining. Shaded grey is control omitting, and black with, GZMB-PE antibody; right, graphical representation; lung n=3, tumor n=12. *P*-value, unpaired Student's t-tests, error bars, S.E.M.; from two experiments. (B) Left, CD71 abundance on sort-purified splenic or tumor-infiltrating CD8$^+$CD44^{high} T cells, both from PyMT mice; right, graphical representation, n=2. Representative of three experiments. (C) *In vitro* photomicrographs of indicated conditions.

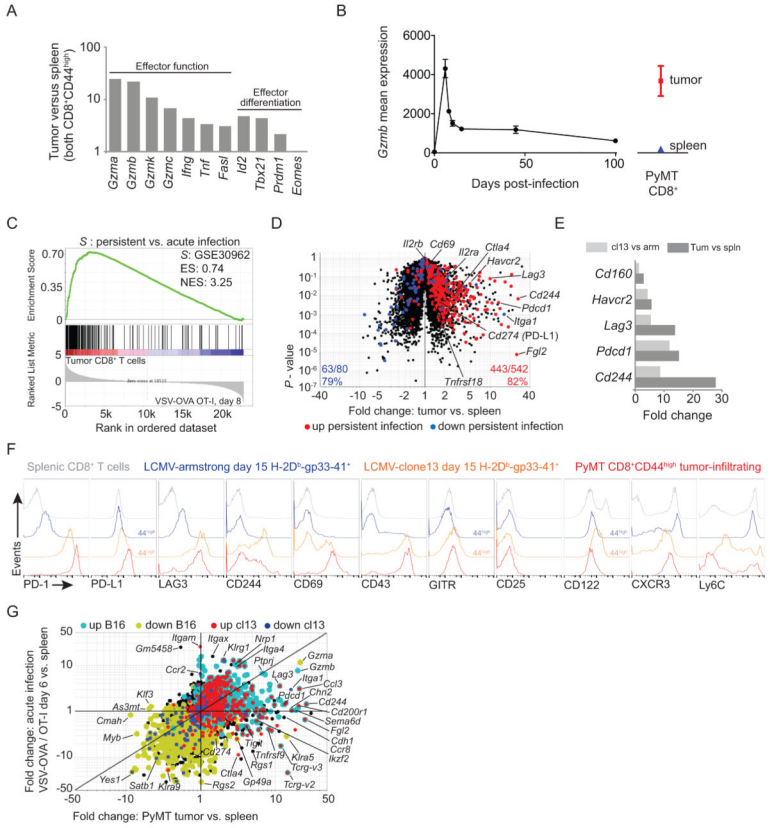

Figure 3. Tumor-infiltrating CD8$^+$ T cells express both abundant effector transcripts and an exhaustion-associated gene-expression signature

(A-E, G) CD8$^+$CD44^{high} T cells sorted from tumors and spleens of PyMT mice; gene expression determined by microarray. (A) Fold change of selected cytotoxic regulators/ effector transcripts. (B) PyMT spleen/tumor CD8$^+$ T-cell microarray data co-normalized with Immgen OT-I/LM-OVA (GSE15907); *Gzmb* transcript abundance in PyMT tumor and splenic CD8$^+$CD44^{high} T cells and virus-specific OT-I CD8$^+$ T cells after LM-OVA infection; expression values directly comparable; error bars S.E.M. (C) Gene set-enrichment analysis (GSEA) of immunologic signatures database using PyMT tumor CD8$^+$ T cells relative to OT-I T cells responding to VSV-OVA, day 8 post-infection (GSE15907). (D) Fold change of PyMT tumor CD8$^+$CD44^{high} relative to splenic CD8$^+$CD44^{high} T cells, plotted versus mean class *P*-value. Highlighted transcripts regulated ≥2-fold in persistent viral infection (persistent versus acute viral infection, day 15; GSE41870). Inset indicates transcripts coordinately up or down ≥2-fold in persistent vs. acute infection and tumor vs. spleen cells. (E) Select exhaustion-associated transcripts (persistent vs. acute infection, day 15; GSE41870) and PyMT tumor versus splenic CD8$^+$CD44^{high}; datasets normalized independently. (F) Indicated molecule abundance on CD8$^+$ T cells by flow cytometry. "CD44^{high}" indicates this gate was used instead of tetramer gate. (G) Fold change versus fold change plot of PyMT tumor CD8$^+$CD44^{high} T cells and OT-I T cells responding to VSV-OVA (day 6), both versus splenic CD8$^+$CD44^{high} T cells from PyMT mice. Transcripts regulated ≥2-fold in persistent versus acute infection, or in B16 melanoma relative to splenic CD8$^+$CD44^{high} T cells, are highlighted.

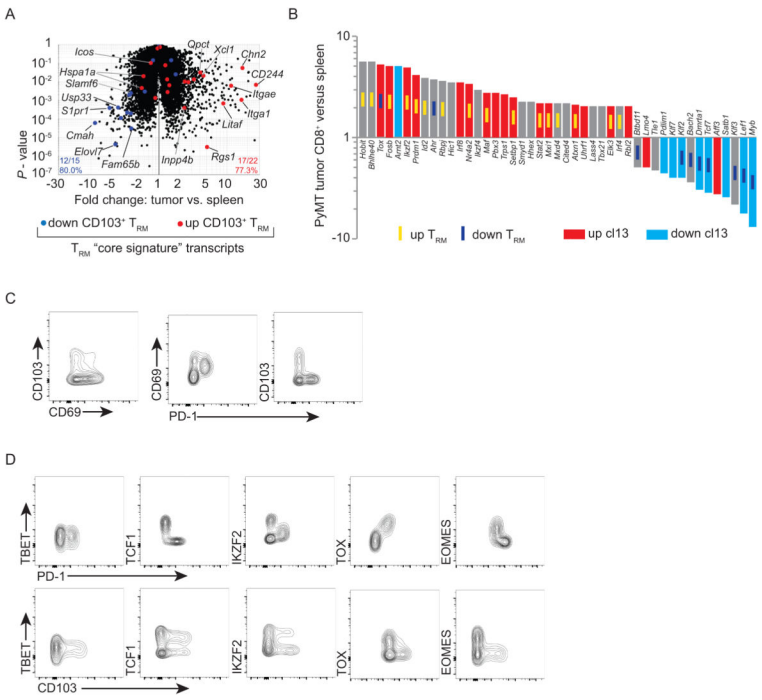

Figure 4. PyMT tumor CD8$^+$ T cells are comprised of distinct exhausted and T_{RM}-like subsets

(A) Fold change vs. *P*-value of PyMT tumor-infiltrating CD8$^+$CD44^{high} T cells versus splenic CD8$^+$CD44^{high} T cell gene expression. "Core T_{RM} signature" transcripts (ref.34) are highlighted; (T_{RM} up, red; T_{RM} down, blue) Inset indicates the fraction and percent of "core T_{RM} signature" genes that are coordinately up or down in T_{RM} and PyMT tumor CD8$^+$ T cells. (B) Transcription factors/regulators up or down ≥2-fold in PyMT CD8$^+$CD44^{high} versus splenic CD8$^+$CD44^{high} T cells. Color-coding of bars indicates whether gene transcript is also up or down in persistent infection, (≥1.3-fold day 15 persistent versus acute infection; GSE41870). Yellow or blue inset bar indicates whether each gene transcript is up/down in tissue-resident memory cells (≥1.3-fold in brain CD103$^+$ T_{RM} versus spleen CD103$^-$ memory cells; GSE39152). PyMT CD8$^+$ T-cell. Gene expression from microarray, as described in Fig.3. (C) Expression of CD103, CD69 and PD-1 on CD8$^+$CD44^{high} PyMT MEC tumor infiltrate. (D) Transcriptional factor/regulator profiling of PyMT tumor CD8$^+$ T cells. Results in C and D representative of three experiments.

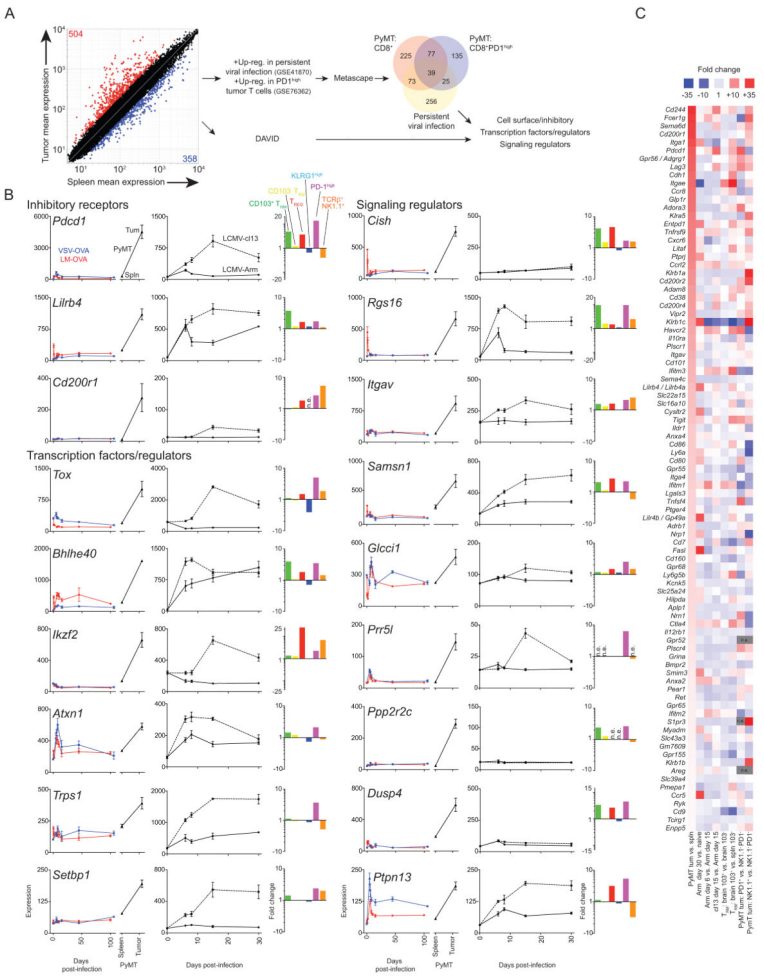

Figure 5. Targeting regulators of tumor CD8$^+$ T-cell responsiveness

(A) Left, mean-class gene expression of PyMT splenic CD8$^+$CD44^{high} versus tumor CD8$^+$CD44^{high} T cells. Inset indicates probesets regulated ≥2-fold, *P*-value < 0.35, expression ≥ 50 in ≥ 3 of the 6 samples. Right, the analysis workflow, and diagram of shared exhaustion-associated transcripts. (B) Gene expression of selected transcripts up-regulated in PyMT tumor CD8$^+$CD44^{high} T cells, error bars indicate S.E.M. Left, expression in pathogen-specific T cells in response to acute infection with VSV-OVA and LM-OVA (GSE15907); plotted on the same *y*-axis and directly comparable, expression in PyMT tumor vs. spleen CD8$^+$CD44^{high} T cells. Middle, independently normalized, virus-specific CD8$^+$ T cell gene expression in response to acute infection (LCMV-Arm) or persistent infection (LCMV-cl13; both GSE41870). Right, fold change of the indicated transcripts in KLRG1^{high}, T_{REG}, T_{RM} (CD103$^+$), T_{RM} (CD103$^-$), tumor CD8$^+$PD1$^+$, or tumor CD8$^+$NK1.1$^+$, relative to control populations. (C) Transcripts up-regulated ≥2-fold in PyMT CD8$^+$CD44^{high} T cells versus spleen for manually collated cell-surface/membrane-associated proteins, ordered highest-to-lowest fold-change. Heat map color-coding is global, lower fold change probesets omitted in cases of duplicates. Data from same sources as in C; datasets normalized independently. For B and C, n.e. indicates fold change not calculated due to poor expression.

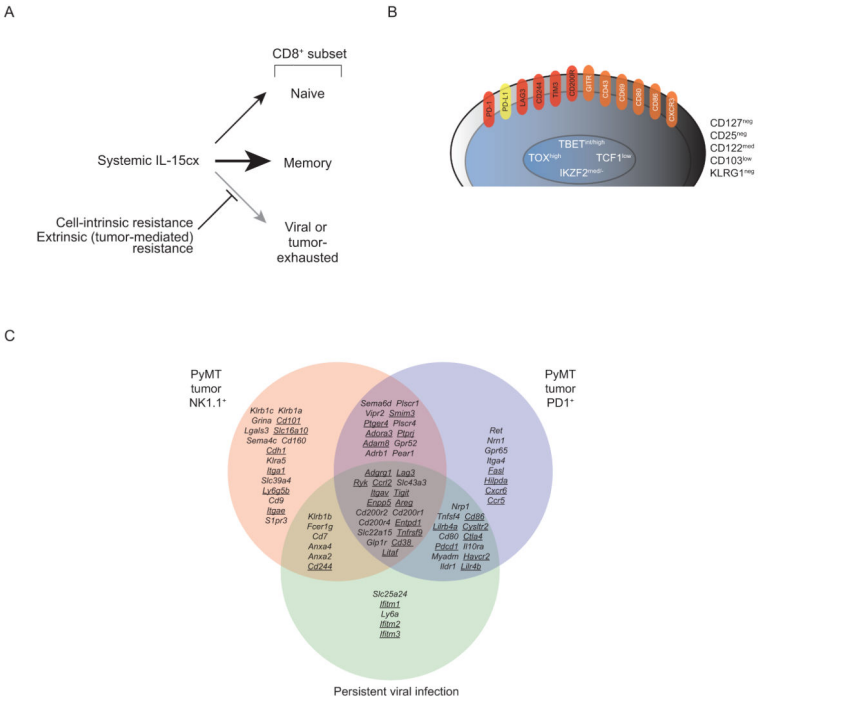

Figure 6. Therapeutic consequences and molecular hallmarks of CD8$^+$ T-cell exhaustion-associated IL15 resistance

(A) Intrinsic and extrinsic factors dampen tumor CD8$^+$ T-cell IL15 responses, leaving systemic IL15cx to primarily activate/expand extra-tumoral CD8$^+$ T cells. (B) Left, partial phenotype of exhausted, IL15-resistant tumor-infiltrating T cell; these proteins validated by flow cytometry in Fig.3,4 and Supplementary Fig. S10. Exhaustion/inhibitory receptors, red; inhibitory ligands, yellow; and other, orange. (C) Cell-surface molecules regulated ≥2-fold or more in PyMT tumor CD8$^+$ T cells versus splenic controls (from Fig. 5C), with transcripts up-regulated ≥1.5 fold in CD8$^+$PD1$^+$ and CD8$^+$NK1.1$^+$ T cells, versus PD1$^-$NK1.1$^-$CD8$^+$ T-cell controls (GSE76362), or in persistent versus acute infection, day 15 (GSE41870). Underlined transcripts are up-regulated ≥1.5-fold in CD103$^+$ brain T_{RM} relative to conventional splenic memory cells (GSE39152).

Table 1

Tumor-infiltating CD8+ T cell functional annotation clusters.

DAVID cluster	Enrichment Score	Cluster Description	# of genes	Selected genes composing cluster
Up-regulated in tumor CD8+ T cells				
1	6.88	Surface/plasma memb.	58	*Pdcd1, Cd38, Ctla4, Ly6a, Adora3, Enpp5, Slc16a10, Itgav*
7	2.65	Neg.reg.signal/G-prt.reg.	13	*Cish, Rgs1, Rgs3, Rgs16, Spry1, Spry2, Socs2, Tgfb3, Atxn1*
8	2.52	SH2 domain	22	*Sh3bp2, Lyn, Chn2, Cish, Clnk, Grb7, Plcg2, Stat2, Vav3*
14	2.61	Ig-like domain cont.	23	*Cd7, Cd80, CD86, Cd160, Cd200r, Lag3, Havcr2, Tigit, Lilrb4*
19	1.78	Phosphatases	12	*Dusp4, Dusp14, Ptpn5, Ptpn7, Ptpn9, Ptpn13, Ptprj, Inpp4a, Inpp4b, Impa2*
Down-regulated in tumor CD8+ T cells				
1	3.06	Transmembrane/recptr.	106	*Cd72, Gpr146, Cd163l1, Cxcr5, Ccr7, Itb3, Tnfrsf10b, Tbxa2r*
3	1.78	Cytokine recptr./recptr.	17	*Btla, CD22, Emb, Il4ra, Il6ra, Il6st, Il7r, Il18r1, Ifngr2*
5	1.55	Ig-like domain cont.	16	*Treml2, Slamf6, Emb, Fcgrt, Icam2, Sell, Pecam1, Sema4f*
10	1.05	Kinases/phosphorylation	57	*Mapk11, Yes1, Dgka, Dusp10, Pik3r5, Ssh2, Stk38, Acp5*